Supporting

Water-stable perovskite-on-polymer fluorescent microspheres for the simultaneous monitoring of pH, urea and urease

Jia An[a, b], Meizhu Chen[a], Guoyi Liu [a, b], Yongqin Hu[a, b], Rubing Chen[a], Ying Lyu[a], Sanjiv Sharma[c], and Yufei Liu[a, b, c *]

[a] Key Laboratory of Optoelectronic Technology & Systems (Chongqing University), Ministry of Education, Chongqing 400044, China

[b] Collaborative Innovation Center for Brain Science, Chongqing University, Chongqing 400044, China

[c] Centre for NanoHealth, College of Engineering, Swansea University, Singleton Park, Swansea SA2 8PP, UK

[*]To whom correspondence should be addressed

Key Laboratory of Optoelectronic Technology & Systems (Chongqing University), Ministry of Education, Chongqing 400044, China

ORCID: 0000-0003-2988-8843

Tel: +86 13522636676

E-mail address: Yufei.Liu@cqu.edu.cn

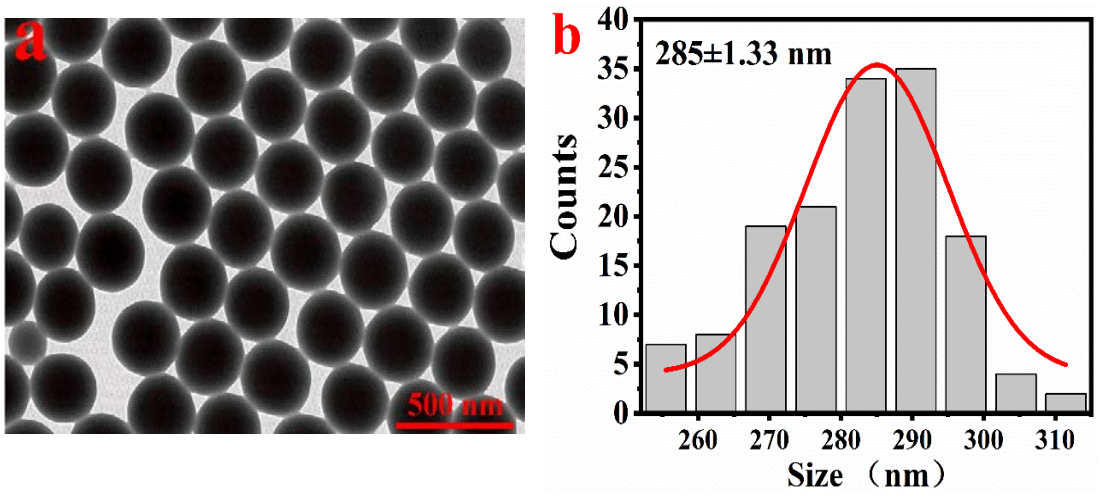

Fig. S1 (a) TEM image of polymer of polystyrene and poly (acrylic acid) (PS-PAA),

(b) Corresponding size distribution of PS-PAA.

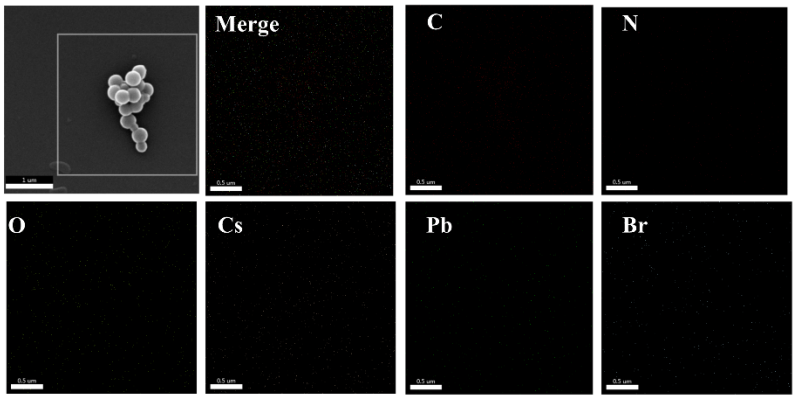

Fig. S2 SEM/EDX elemental mapping analysis of the synthesized PDPS composites.

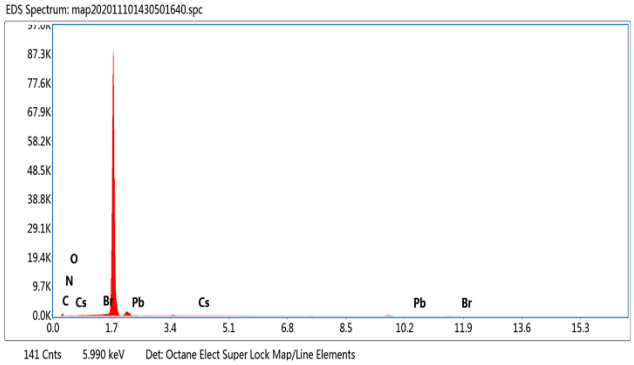

Fig. S3 The corresponding EDX images of PDPS composites.

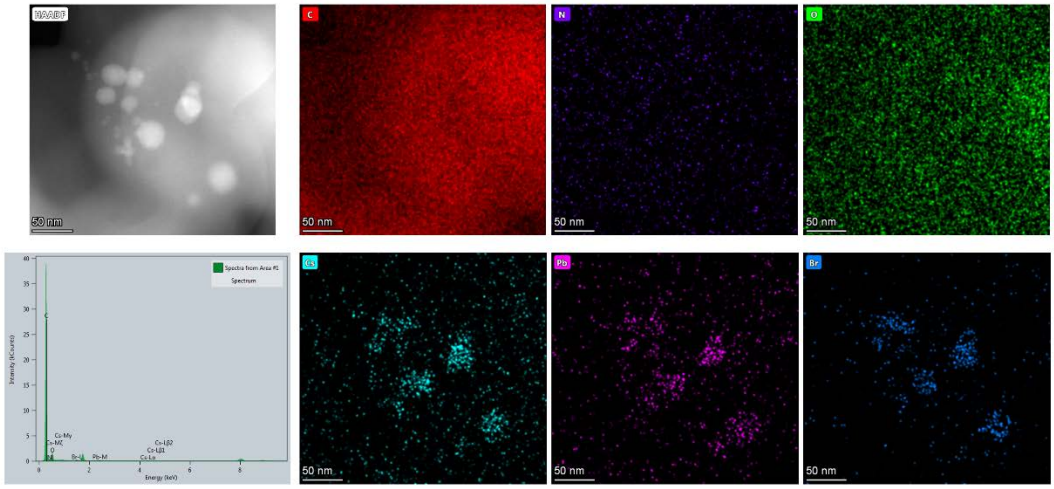

Fig. S4 The HAADF-STEM image and corresponding EDS layered images of the PDPS composites.

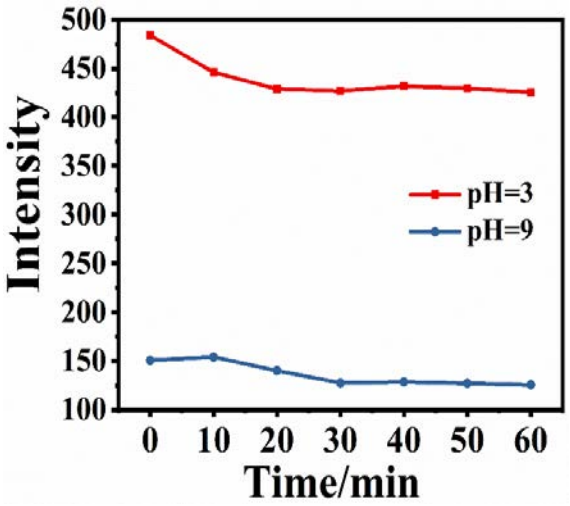

Fig. S5 Fluorescent intensity (λex=300 nm) of the PDPS composites with different reaction time.

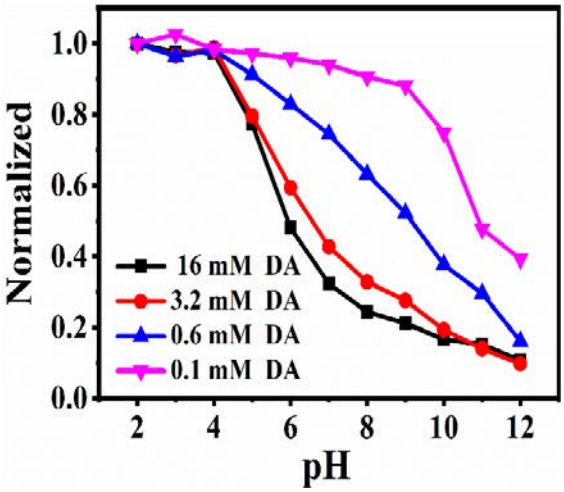

Fig. S6 The relationship between fluorescent intensity of the PDPS composites and pH at different concertation of DA

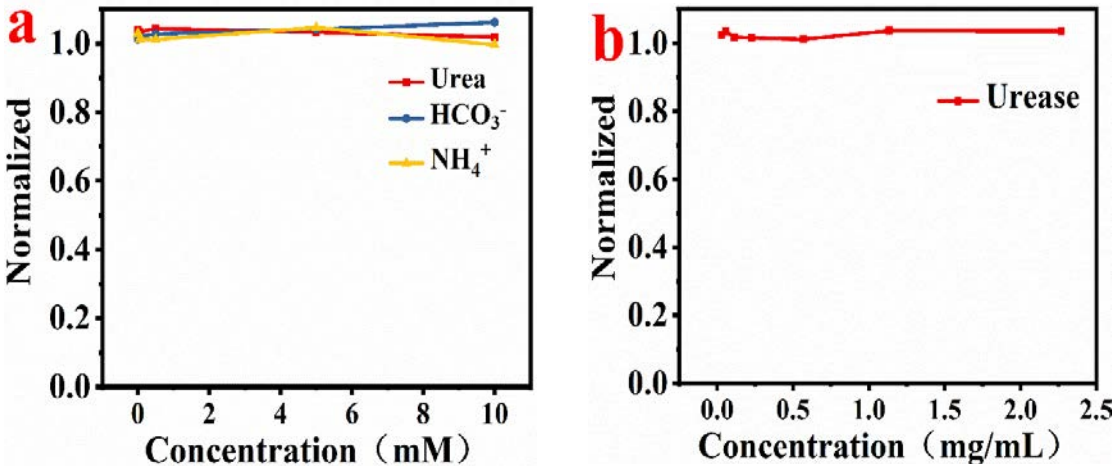

Fig. S7 The fluorescent intensity of the PDPS composites at different concertation of (a) Urea, HCO_3^-, NH_4^+, (b) Urease.

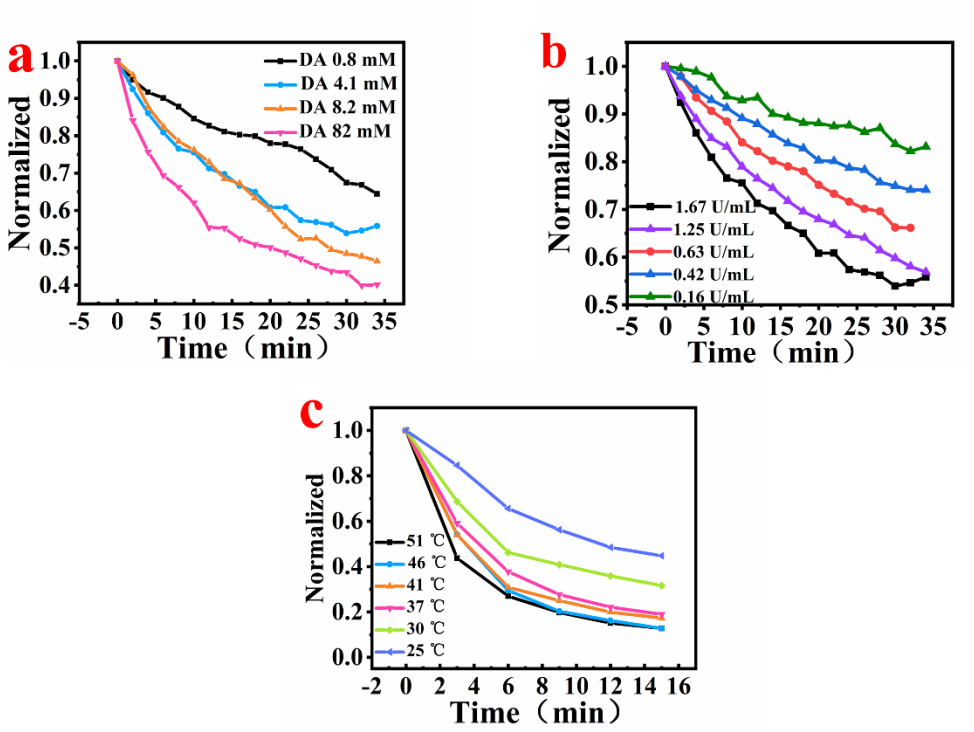

Fig. S8 The relationship between fluorescent intensity of the PDPS composites and the reaction time at different concertation of (a) DA, (b) Urease, (c) Temperature.

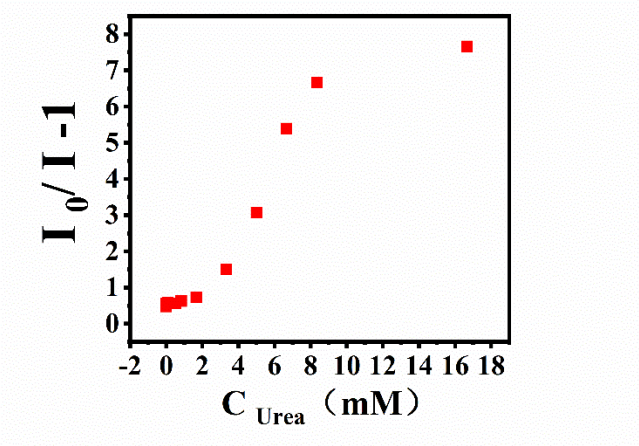

Fig. S9 The linear relationship between (I_0/I-1) and urea concentration.

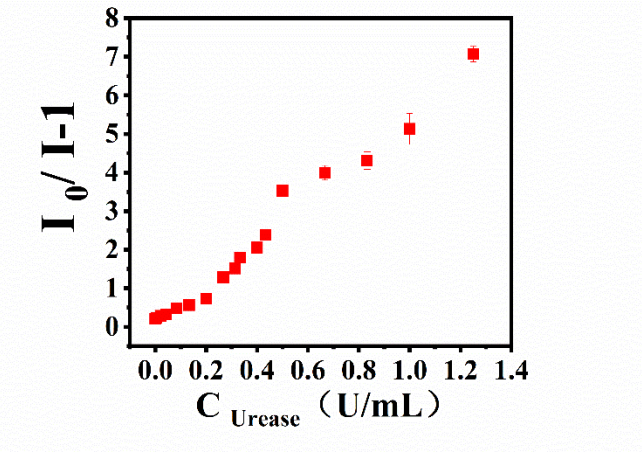

Fig. S10 The linear relationship between (I_0/I-1) and urease concentration.

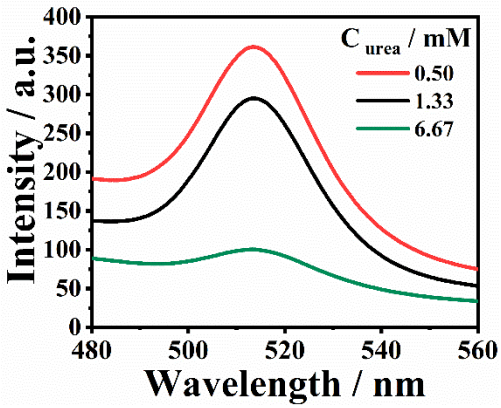

Fig.S11 Fluorescent emission spectra (λex=300 nm) of the PDPS composites with different concentrations of urea in real human serum samples.

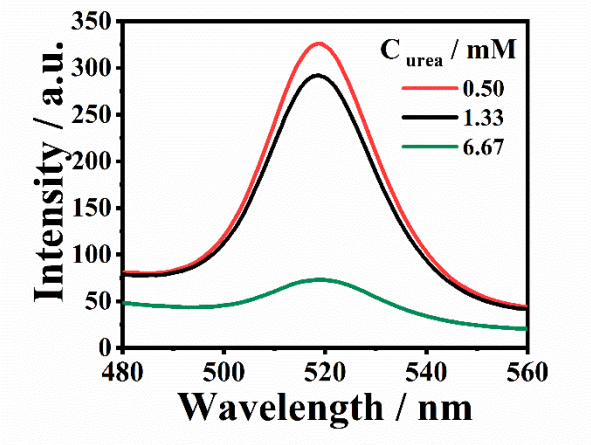

Fig.S12 Fluorescent emission spectra (λex=300 nm) of the PDPS composites with different concentrations of urea in real human urine samples.

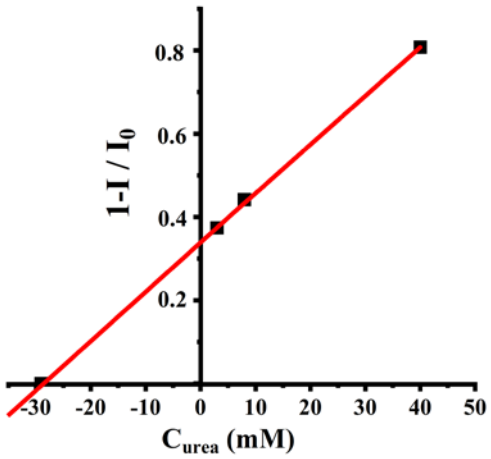

Fig.S13 Standard addition approach graph of detecting unknown concentrations of urea in real human serum samples.

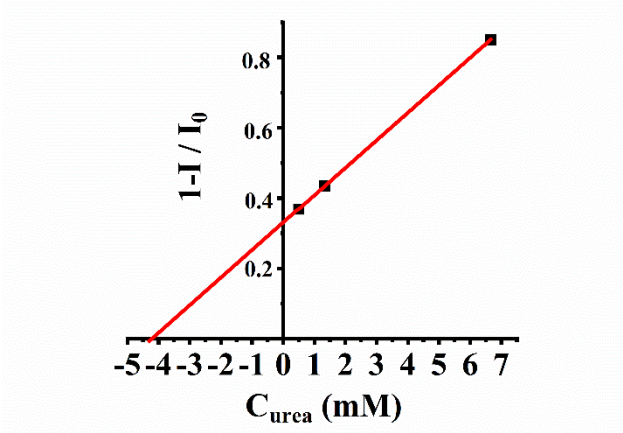

Fig.S14 Standard addition approach graph of detecting unknown concentrations of urea in real human serum samples.

Table S1

The comparison for urea detection among different sensors.

Type	Materials	Response time	Linear range	Detection limit	References

Electrochemistry	Yb_2O_3	-	0.05-19 mM	2 μM	[4]
Fluorescence	P dots	45 min	0 -1 mM	0.02 mM	[5]
Fluorescence	CuO NPs	45 min	0.0375-0.3 mM	27 μM	[6]
Electrochemistry	MWCNT-PoT	-	0.1-11 mM	0.03 mM	[7]
Phosphorescence	MPA-CdTe quantum dots	10 min	0.016-0.16 mM	0.003 mM	[8]
Electrochemistry	urease/SF/aminated GCE	-	0.3-2.7 mM	0.163 mM	[9]
Fluorescence	MoS_2 QDs	44 min	5-700 μM	1.8 μM	[10]
Fluorescence	PDPS composites	30 min	1.67 μM-6.67 mM	1.67 μM	This work

Table S2

The comparison of constructed sensor with other perovskite-based sensors.

Materials	Analyte	Signal	Stability	Detection Condition	References
$CsPbBr_3$	Picric acid	Fluorescence	Vulnerable to humidity /pH/temperature	Cyclohexane	[11]
$CsPbBr_3$/cellulose composites	Chloride and Iodide Ions	Absorbance	Vulnerable to humidity /pH/temperature	Water	[12]
$CH_3NH_3PbBr_3$	Hg^{2+}	Fluorescence	Vulnerable to humidity /pH/temperature	Toluene	[13]
$CsPbBr_3$	Cu^{2+}	Fluorescence	Vulnerable to humidity /pH/temperature	Cyclohexane	[14]
$(C_6H_5NH_3)_2Pb_3I_8 \cdot 2H_2O$	Fe^{3+}	Fluorescence	Vulnerable to humidity /pH/temperature	DMF	[15]
$CsPbBr_3$/MIP	Pesticide	Fluorescence	Vulnerable to humidity /pH/temperature	Dichloromethane	[16]
PDPS composites	pH/urea/urease	Fluorescence	Hyperstatic	Water	This work

References

1. Song J, Li J, Xu L, Li J, Zhang F, Han B et al. Room-Temperature Triple-Ligand Surface Engineering Synergistically Boosts Ink Stability, Recombination Dynamics, and Charge Injection toward EQE-11.6% Perovskite QLEDs. Adv Mater. 2018;30(30):e1800764. http://doi:10.1002/adma.201800764.

2. Protesescu L, Yakunin S, Bodnarchuk MI, Krieg F, Caputo R, Hendon CH et al. Nanocrystals of Cesium Lead Halide Perovskites (CsPbX3, X = Cl, Br, and I): Novel Optoelectronic Materials Showing Bright Emission with Wide Color Gamut. Nano Letters. 2015;15(6):3692-6. http://doi:10.1021/nl5048779.

3. Xie HY, Zuo C, Liu Y, Zhang ZL, Pang DW, Li XL et al. Cell-targeting multifunctional nanospheres with both fluorescence and magnetism. Small. 2005;1(5):506-9. http://doi:10.1002/smll.200400136.

4. Ibrahim AA, Ahmad R, Umar A, Al-Assiri MS, Al-Salami AE, Kumar R et al. Two-dimensional ytterbium oxide nanodisks based biosensor for selective detection of urea. Biosens Bioelectron. 2017;98:254-60. http://doi:10.1016/j.bios.2017.06.015.

5. Huang H, Li J, Liu M, Wang Z, Wang B, Li M et al. pH-controlled fluorescence changes in a novel semiconducting polymer dot/pyrogallic acid system and a multifunctional sensing strategy for urea, urease, and pesticides. Analytical Methods. 2017;9(47):6669-74. http://doi:10.1039/c7ay02284k.

6. Deng HH, Zheng XQ, Wu YY, Shi XQ, Lin XL, Xia XH et al. Alkaline peroxidase activity of cupric oxide nanoparticles and its modulation by ammonia. Analyst. 2017;142(20):3986-92. http://doi:10.1039/c7an01293d.

7. Hassan RYA, Kamel AM, Hashem MS, Hassan HNA, Abd El-Ghaffar MA. A new disposable biosensor platform: carbon nanotube/poly(o-toluidine) nanocomposite for direct biosensing of urea. Journal of Solid State Electrochemistry. 2018;22(6):1817-23. http://doi:10.1007/s10008-017-3857-z.

8. Oymak T, Ertaş N, Tamer U. Use of Water Soluble and Phosphorescent MPA Capped CdTe Quantum Dots for Detection of Urea. The Turkish Journal of Pharmaceutical Sciences. 2018;15(1):44-9. http://doi:10.4274/tjps.02986.

9. Rafiq K, Mai HD, Kim JK, Woo JM, Moon BM, Park CH et al. Fabrication of a highly effective electrochemical urea sensing platform based on urease-immobilized silk fibroin scaffold and aminated glassy carbon electrode. Sensors and Actuators B: Chemical. 2017;251:472-80. http://doi:10.1016/j.snb.2017.05.048.

10. Zhang F, Wang M, Zhang L, Su X. Ratiometric fluorescence system for pH sensing and urea detection based on MoS2 quantum dots and 2, 3-diaminophenazine. Anal Chim Acta. 2019;1077:200-7. http://doi:10.1016/j.aca.2019.06.001.

11. Chen X, Sun C, Liu Y, Yu L, Zhang K, Asiri AM et al. All-inorganic perovskite quantum dots CsPbX3 (Br/I) for highly sensitive and selective detection of explosive picric acid. Chem Eng J. 2020;379:122360. http://doi:10.1016/j.cej.2019.122360.

12. Park B, Kang S-M, Lee G-W, Kwak CH, Rethinasabapathy M, Huh YS. Fabrication of CsPbBr3 Perovskite Quantum Dots/Cellulose-Based Colorimetric Sensor: Dual-Responsive On-Site Detection of Chloride and Iodide Ions. Industrial & Engineering Chemistry Research. 2019;59(2):793-801. http://doi:10.1021/acs.iecr.9b05946.

13. Lu LQ, Tan T, Tian XK, Li Y, Deng P. Visual and sensitive fluorescent sensing for ultratrace mercury ions by perovskite quantum dots. Anal Chim Acta. 2017;986:109-14.

http://doi:10.1016/j.aca.2017.07.014.
14. Sheng X, Liu Y, Wang Y, Li Y, Wang X, Wang X et al. Cesium Lead Halide Perovskite Quantum Dots as a Photoluminescence Probe for Metal Ions. Adv Mater. 2017;29(37). http://doi:10.1002/adma.201700150.
15. Zhu M-Y, Zhang L-X, Yin J, Chen J-J, Bie L-J. A fluorescence quenching sensor for Fe3+ detection using (C6H5NH3)2Pb3I8·2H2O hybrid perovskite. Inorg Chem Commun. 2019;109:107562. http://doi:10.1016/j.inoche.2019.107562.
16. Tan L, Guo M, Tan J, Geng Y, Huang S, Tang Y et al. Development of high-luminescence perovskite quantum dots coated with molecularly imprinted polymers for pesticide detection by slowly hydrolysing the organosilicon monomers in situ. Sensors and Actuators B: Chemical. 2019;291:226-34. http://doi:10.1016/j.snb.2019.04.079.